Proceedings of the International Symposium on Physics of Materials (ISPMA13)

Atom Probe Tomography Investigations of Modified Early Stage Clustering in Si-Containing Aluminum Alloys

S. Pogatscher[a,*], S.S.A. Gerstl[b], J.F. Löffler[a] and P.J. Uggowitzer[a]

[a]Laboratory of Metal Physics and Technology, Department of Materials, ETH Zurich, Switzerland

[b]Scientific Center of Optical and Electron Microscopy, ETH Zurich, Switzerland

In this paper atom probe tomography is used to explore early stage clustering in aluminum alloys. Two novel concepts for a modification of clustering are discussed. Control of early stage clustering is welcome from an application point of view since clustering deteriorates strength evolution during the industrial heat treatment of the important class of Al–Mg–Si precipitation-hardenable alloys. Nanoscale early stage clusters are very difficult to observe and atom probe tomography is the best technique to visualize and chemically measure Si or Mg-containing clusters in aluminum alloys. Restrictions remain in achieving the ultimate quantification of such small solute aggregates by atom probe tomography, such as detection efficiency, local magnification effects, surface migration of solute atoms, and unresolved issues with the reconstruction procedure. Here we investigate one of these restricting effects, namely the migration of solute atoms during atom probe tomography measurements. In particular Si is found to be preferentially localized or absent at certain crystallographic poles in aluminum, which derogates the experimental results gained from atom probe tomography studies of clustering in Si-containing aluminum alloys. This artifact is investigated for different specimen temperatures, detection rates and pulse fractions during atom probe tomography measurements. Optimal strategies to analyze small-scale solute clusters in Si-containing aluminum alloys are presented.

DOI: 10.12693/APhysPolA.128.643

PACS: 64.70.kd, 61.72.–y, 81.40.Gh

1. Introduction

Al–Mg–Si alloys are the most frequently used age-hardenable aluminum alloys, with applications in construction, cars, aircrafts and architecture [1]. Early-stage clustering at room temperature (RT) after quenching has emerged as a research field in this class of alloys in recent years, because it deteriorates the applied industrial hardening strategies and the resulting properties [2–4]. From an academic point of view little is known about this solute clustering [4]. In general, the mobile quenched-in vacancy concentration is important for kinetics of all diffusion-controlled processes which occur at low temperatures, i.e. clustering at RT. Recently, two strategies of modifying clustering in Al–Mg–Si alloys have been introduced. Firstly, interrupted quenching can significantly reduce the overall excess-vacancy concentration (V) and consequently decrease the clustering kinetics [5]. Secondly, trace additions of Sn can be utilized to trap excess-vacancies and hence reduce the mobile vacancy concentration, which also decreases clustering kinetics [6]. Figure 1 shows a schematic illustration of these concepts.

To explore the occurring changes in clustering upon the above-discussed strategies, appropriate tools are required to increase the physical understanding of the processes occurring at the atomic length scale. A visualization of clusters is difficult because transmission electron microscopy does not produce distinct contrast [4, 7].

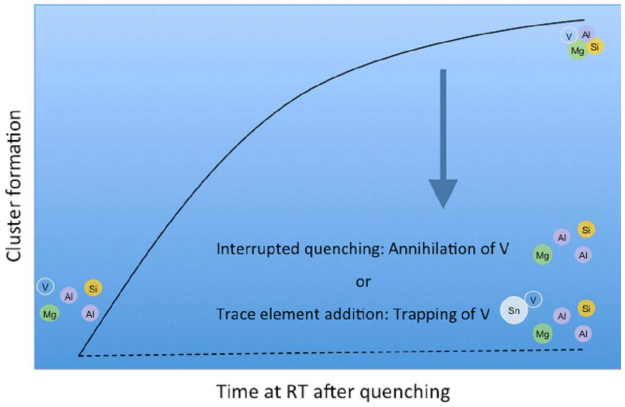

Fig. 1. Schematic illustration of the suppression of room-temperature clustering in Al–Mg–Si alloys via interrupted quenching and trace element additions.

The low alloying-element content also implies a low signal-to-noise ratio for any element-sensitive probe, and Mg, Al and Si are of similar atomic number, generating very similar signal for various scattering techniques [4]. Today atom probe tomography (APT) is the best technique to visualize and chemically measure Si or Mg-containing clusters in aluminum alloys; accordingly, there are numerous APT studies on clustering in Al–Mg–Si alloys. References [7–15] provide an overview of established papers in the field and references [5, 6, 16–18] are recent papers on the topic. In many cases number densities and the chemical composition of different types of clusters are determined. However, restrictions in quantifying small solute aggregates by APT, such as detection efficiency of the instruments (40% to 60%, depending on the

*corresponding author; e-mail: Stefan.Pogatscher@unileoben.ac.at

type of atom probe), local magnification effects, surface migration of solute atoms, and unresolved issues with assumptions of the reconstruction procedure are not discussed in a detailed manner in many cases, or references are cited which peripherally (or on different materials systems) address these issues.

In this study we investigate one of these restricting effects, namely the migration of solute atoms during APT measurements. Si is found to preferentially migrate to certain crystallographic poles in Al–Mg–Si alloys, which derogates the experimental results gained from APT studies of clustering in Si-containing aluminum alloys. We also investigate the effect for different APT parameters (specimen temperature, detection rate, pulse fraction) in a pure binary Al–Si solid solution and present optimal strategies and APT parameters to analyze aluminum alloys with low alloying amount of Si.

2. Experimental

To illustrate the artifact we first utilized a supersaturated pure ternary Al0.33Si0.29Mg alloy (all concentration values given in at.%) and then studied the impact of different APT measurement parameters in a supersaturated pure binary Al0.69Si alloy.

Needle-shaped APT specimens were prepared via a standard two-step method [19]: after initial electropolishing of the samples with 10% perchloric acid and 90% methanol solution, 2% perchloric acid in butoxyethanol was used as the second electrolyte. APT measurements were performed on a LEAP™ 4000 X HR with specimen temperatures from 20 K to 60 K; pulse fractions (PF) from 15% to 25%; various detection rates (DR) between 0.5% to 1.5%; and a pulse rate of 200 kHz under ultra-high vacuum ($< 10^{-10}$ mbar) conditions. The software package IVAS 3.6.6™ from Cameca was employed for the reconstruction procedure and analysis.

3. Results and discussion

Detector hit maps (DHMs, cumulative hit positions of ions on the detector) of alloys with low levels of solutes show a pattern that is characteristic of the crystallography and specific orientation of the APT sample [20]. Figure 2a illustrates such a map for the alloy Al0.33Si0.29Mg measured at 20 K, with a pulse fraction of 20% and a detection rate of 1%. The hit density varies from dark (low hit density; typically revealing crystallographic poles and zone lines) to bright (high hit density). The crystallographic poles are also indicated in Fig. 2a.

Figure 2b,c shows Mg and Si positions superimposed on a two-dimensional density map of Al, which enables a quick identification of the crystallographic details. Analogously to the DHM the Al density varies from dark (low density) to bright (high density). The distribution of Mg, black in Fig. 2b, appears quite homogeneous. In the case of Si this is not the case. Si is highly enriched at the 111 pole and its adjacent zone lines (Fig. 2c). As this is a low-density region of Al, the measured Si concentration

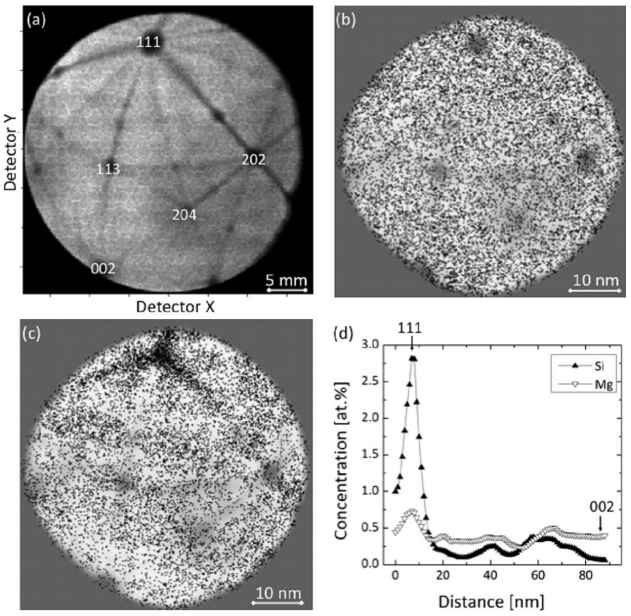

Fig. 2. APT data of Al0.33Si0.29Mg. (a) Detector hit map. (b,c) Distribution of (b) Mg and (c) Si superimposed on a two-dimensional density map of Al. (d) Linear concentration profile from the 111 pole to the 002 pole.

will be far too high in that region, whereas some other poles show a depletion of Si (see 002 pole). Figure 2d shows a concentration line profile from the 111 pole to the 002 pole. An increase in Si concentration at the 111 pole and a decrease in Si concentration at the 002 pole are obvious. There is also an artifact for Mg, but it is much less pronounced.

Field gradients at the APT tip surface can cause a thermally activated migration of certain solute atoms [21]. The effect is known from field ion microscopy (e.g. [22]) and has been recently quantified for APT for a variety of solutes in Fe alloys [20]. Solute atoms with an evaporation field significantly higher than the matrix can remain on the tip and migrate over the surface (for Al–Mg–Si alloys: $Al^{+} = 19$ V/nm, $Si^{++} = 33$ V/nm, $Mg^{+} = 21$ V/nm, image hump model values from [21]). These differences may be the reason for the observed behavior in Fig. 2. The evaporation field of Mg is close to that of Al, and Mg does not show a very pronounced migration artifact. The evaporation field of Si is significantly higher than that of Al, and Si tends to evaporate at high field positions. Interestingly, a shift from the 002 pole towards the 111 pole has also been observed for Ag-containing precipitates in Al–Ag alloys ($Ag^{+} = 24$ V/nm) [23].

In particular, if Si-containing clusters are studied in Al alloys, it is critical to minimize the influence of this artifact. A statistical analysis of Si atom positions [24] at the wrong position in such dataset (i.e. 111 pole) would reveal a non-random behavior for a material that exhibits a random solute distribution in reality. A study of Mg in Al–Mg–Si alloys is easier and more appropriate even

without paying too much attention to this point. However most studies, which show APT on clusters in Al–Mg–Si results do not outright discuss these artifacts, although the authors might have considered them in their analysis.

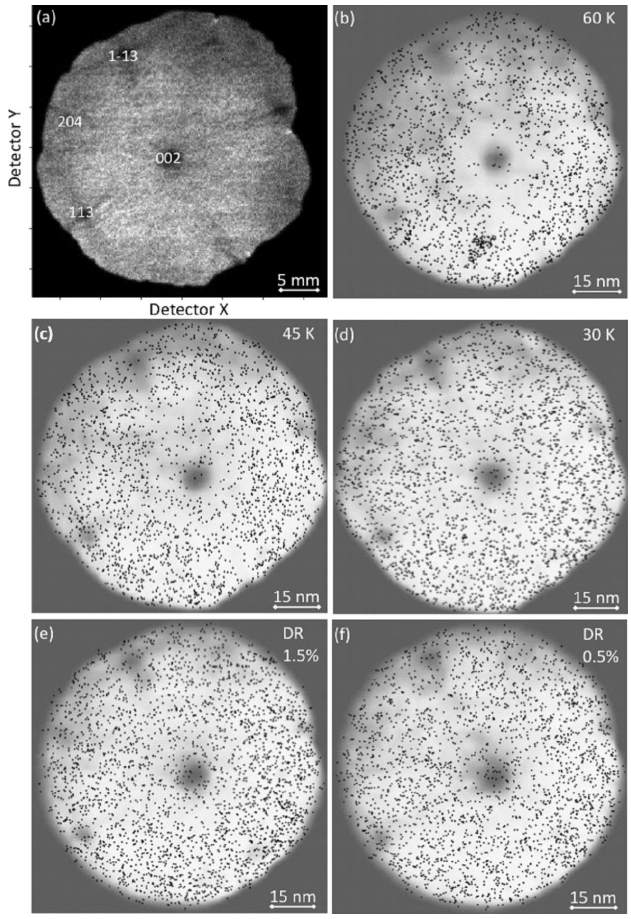

Fig. 3. Influence of APT parameters in Al0.69Si. (a) Detector hit map. (b)–(f) Distribution of Si superimposed on a two-dimensional density map of Al for a specimen temperature of (b) 60 K, (c) 45 K, and (d) 30 K with 1% DR and 20% PF. Variation of the DR to (e) 1.5% and (f) 0.5% at 30 K and 20% PF.

Figure 3 investigates the influence of APT parameters (specimen temperature and detection rate) for Al0.69Si alloy. The DHM (Fig. 3a) shows that the grain of the specimen is in a different orientation compared to Fig. 2 since a 111 pole is not present. Nevertheless, Fig. 3b–f reveal the migration of Si towards or away from crystallographic poles during the measurement. The effect of the temperature is pronounced and higher temperatures lead to stronger migration, which is in accordance with the reported thermally activated character of surface migration [20]. Around the 002 pole a very low density of Si is observed at 60 K. Lower specimen temperature minimizes the artifact. The DR does not considerably affect the migration of Si at 30 K.

Figure 4 investigates the influence of the pulse fraction for Al0.69Si. Figure 4b–d does not reveal strongly

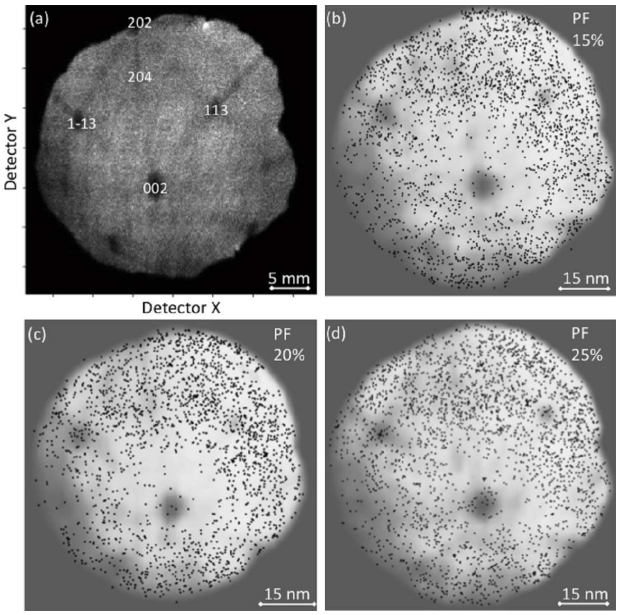

Fig. 4. Influence of APT parameters in Al0.69Si. (a) Detector hit map. (b)–(d) Distribution of Si superimposed on a two-dimensional density map of Al for a PF of (b) 15%, (c) 20%, and (d) 25% with 1% DR and a temperature of 30 K.

pronounced differences in the migration of Si atoms during the measurement. It seems to be a trend that a high PF slightly reduces it. Note that the background noise level was reduced by decrease of the specimen temperature and increase of DR and PF, as it is generally expected [25].

TABLE

Influence of APT parameters on the Si content measured in Al0.69Si.

Parameters	Si [at.%]
60 K, 1% DR, 20% PF	0.48
45 K, 1% DR, 20% PF	0.59
30 K, 1% DR, 20% PF	0.65
30 K, 1.5% DR, 20% PF	0.65
30 K, 0.5% DR, 20% PF	0.60
30 K, 1% DR, 15% PF	0.56
30 K, 1% DR, 20% PF	0.64
30 K, 1% DR, 25% PF	0.65

Compositional measurements of Al–Mg–Si alloys via APT have been shown to be influenced by the applied parameters [26]. The measured compositions for Al0.69Si are summarized for all investigated parameters in the Table for APT data for regions which do not include major crystallographic poles or zone lines according to the DHMs. With increasing temperature the measured Si-concentration decreases. The PF and the DR have a smaller, but also noticeable effect on the chemical composition determined and a high PF appears to be desirable to reduce the artifact. The whole datasets of Figs. 3

and 4 may be influenced by the 002 pole, which shows a considerable depletion in Si. A different crystallographic orientation of the sample might change the situation [26]. Thus, great care has to be taken when analyzing Si-containing aluminum alloys. Regions with major crystallographic poles or zone lines should be generally cut out, and 002 and 111 poles should be avoided in particular. Low specimen temperature should generally be used, and high pulse fraction and detection rate are favorable to generate high-quality APT data.

4. Conclusions

In summary, we have shown that an investigation of solute clustering of Si in Al–Mg–Si alloys needs a correct adjustment of atom probe tomography parameters and a careful treatment of the acquired data.

- At the 002 pole a depletion of Si can be found, while the 111 pole is strongly enriched in Si.
- Thermally activated field-induced surface migration is suggested as possible mechanism.
- The specimen temperature should be as low as possible to minimize thermal activated Si migration (e.g. 20 K).
- Exclusion of highly affected crystallographic regions of APT datasets is necessary for appropriate solute analysis.

Acknowledgments

The authors thank the AMAG Rolling for the financial support of this work. We also thank P. Schumacher and B. Milkereit from the University of Rostock for providing the Al0.69Si alloys.

References

[1] C. Kammer, *Aluminium Handbook*, Beuth, Berlin 2011.

[2] C.D. Marioara, S.J. Andersen, J.E. Jansen, H.W. Zandbergen, *Acta Mater.* **51**, 789 (2003).

[3] S. Pogatscher, H. Antrekowitsch, H. Leitner, T. Ebner, P.J. Uggowitzer, *Acta Mater.* **59**, 3352 (2011).

[4] J. Banhart, C.S.T. Chang, Z.Q. Liang, N. Wanderka, M.D.H. Lay, A.J. Hill, *Adv. Eng. Mater.* **12**, 559 (2010).

[5] S. Pogatscher, E. Kozeschnik, H. Antrekowitsch, M. Werinos, S.S.A. Gerstl, J.F. Löffler, P.J. Uggowitzer, *Scr. Mater.* **89**, 53 (2014).

[6] S. Pogatscher, H. Antrekowitsch, M. Werinos, F. Moszner, S.S.A. Gerstl, M.F. Francis, W.A. Curtin, J.F. Löffler, P.J. Uggowitzer, *Phys. Rev. Lett.* **112**, 225701 (2014).

[7] J. Buha, R.N. Lumley, A.G. Crosky, K. Hono, *Acta Mater.* **55**, 3015 (2007).

[8] M. Murayama, K. Hono, M. Saga, M. Kikuchi, *Mater. Sci. Eng.* **250**, 127 (1998).

[9] M. Murayama, K. Hono, *Acta Mater.* **47**, 1537 (1999).

[10] D. Vaumousse, A. Cerezo, P.J. Warren, *Ultramicroscopy* **95**, 215 (2003).

[11] F. De Geuser, W. Lefebvre, D. Blavette, *Philos. Mag. Lett.* **86**, 227 (2006).

[12] G.A. Edwards, K. Stiller, G.L. Dunlop, M.J. Couper, *Acta Mater.* **46**, 3893 (1998).

[13] M. Murayama, K. Hono, W.F. Miao, D.E. Laughlin, *Metall. Trans. A* **32**, 239 (2001).

[14] A. Serizawa, S. Hirosawa, T. Sato, *Metall. Trans. A* **39**, 243 (2008).

[15] C.S.T. Chang, I. Wieler, N. Wanderka, J. Banhart, *Ultramicroscopy* **109**, 585 (2009).

[16] P.A. Rometsch, L.F. Cao, X.Y. Xiong, B.C. Muddle, *Ultramicroscopy* **111**, 690 (2011).

[17] L. Cao, P.A. Rometsch, M.J. Couper, *Mater. Sci. Eng. A* **559**, 257 (2013).

[18] R.K.W. Marceau, A. De Vaucorbeil, G. Sha, S.P. Ringer, W.J. Poole, *Acta Mater.* **61**, 7285 (2013).

[19] M.K. Miller, A. Cerezo, M.G. Hetherington, G.D.W. Smith, *Atom Probe Field Ion Microscopy*, Oxford University Press, Oxford 1996.

[20] B. Gault, F. Danoix, K. Hoummada, D. Mangelinck, H. Leitner, *Ultramicroscopy* **113**, 182 (2012).

[21] B. Gault, M.P. Moody, J.M. Cairney, S.P. Ringer, *Atom Probe Microscopy*, Springer, New York 2012.

[22] R. Gomer, *Rep. Prog. Phys.* **53**, 917 (1990).

[23] E.A. Marquis, F. Vurpillot, *Microsc. Microanal.* **14**, 561 (2008).

[24] E.A. Marquis, J.M. Hyde, *Mater. Sci. Eng. R* **69**, 37 (2010).

[25] D.J. Larson, T.J. Prose, R.M. Ulfig, B.P. Geiser, T.F. Kelly, *Local Electrode Atom Probe Tomography*, Springer, New York 2013.

[26] F. Danoix, M.K. Miller, A. Bigot, *Ultramicroscopy* **89**, 177 (2001).